https://doi.org/10.2352/CIC.2022.30.1.17

Visibility Improvement in Air Pollution Scene by Joint Sharpness - Contrast Enhanced Dehazing

Hiroaki Kotera; Kotera Imaging Laboratory, Chiba, Japan

Abstract

In the latter half of the 1980s, PM2.5 pollution in Beijing became a serious problem, and there were concerns about health hazards. It was expected that China's emissions must be reduced from 2013 to 2016, and the lockdown effect of Covid-19 would bring about an end, but it is still reluctant to regulate CO2 emissions. Again, in Beijing in November 2021, a visibility of 500 m or less has been observed, then road traffic is dangerous in addition to health.

After that, the center of pollution has moved from India to Mongolia, and now Nepal, Qatar and Saudi Arabia. The situation is still serious in developing countries.

Image restoration to remove the effects of haze and fog has been a long-standing concern of NASA, and their original Visual Servo has been put into practical use. Though the mainstream moved to the technique based on atmospheric physics. He et al.'s Dark Channel Priority (DCP) logic has had a certain effect on heavily polluted PM 2.5 scenes , but there is a limit to the restoration of detailed visibility. The observed images are affected by two spatial inhomogeneities of 1) atmospheric layer and 2) illumination.

As a countermeasure, we have improved DCP process with the help of Retinex and introduced the veil coefficient as reported in CIC24. Recently, a variety of improvements in single image Dehazing, using FFA-net, BPP-net, LCA-net, or Vision-based model are in progress. However, in each case, visibility of details is still a common problem.

This paper proposes an improvement in detail visibility by
(1) joint sharpness-contrast preprocess
(2) adjustment in Dehaze effect with veil coefficient v

Lastly, we challenge numerical evaluation of improvement in detail visibility by the two ways of attenuation of high-frequency Fourier spectrum and the expansion rate of the color gamut.

Background

The center of air pollution caused by PM2.5 has moved from Beijing to India, Mongolia, Nepal, Qatar, and Saudi Arabia, and the world's death toll continues to be over 7 million annually (WHO report, Oct. 2021).

In everyday scenes, the visibility of dark areas in the shade of trees and buildings is significantly reduced. Even in fine weather, it is affected by attenuation and scattering by the atmospheric layer. The former is due to the illumination light, and the latter is due to the spatial inhomogeneity of the atmospheric transmittance.

Image restoration methods that eliminate the effects of haze or fog have long been a concern at NASA. The *Langley Institute* has evolved a visual model [4] based on *Retinex* [1][2][3] into an advanced method called *Visual Servo* [5] based on a large amount of statistical analysis. However, unlike NASA, Dehazing which excludes the effects of haze or fog, mainly uses algorithms based on atmospheric physics [6] ~[9], and there are many reports [10] ~ [21].

Key Approaches

The key to removing the influence of the air polluted layer based on the atmospheric physics model was the estimation of the transmittance of the scene. In the atmospheric physics model the observed deterioration images are mainly influenced by
1) Attenuation of light reflected from the subject by atmosphere
2) Superimposition of scattered light by the atmosphere (veil).

In the previous reports [13] ~ [15], the author proposed a simplified model with reference to the method of He et al. [10], and made improvements summarized in the following two ***key*** points.
key1 *Estimating the* ***skylight*** that will be the scene illumination
key2 *Smooth estimation of scene* ***transmittance***

For ***key1***, the same performance as He et al., was obtained by a simplified method using only the luminance channel.

As for ***key2***, the Soft matting process using the Laplacian matrix by He et al., needs high computational costs and is complicated, so the smoothing filter that preserves the edges is simplified as an alternative. The effect is comparable to that of other typical methods.

In the follow-up report [16], Dehaze and Retinex were mobilized to improve the visibility of everyday scenes where the *atmospheric layer* and the *spatial inhomogeneity* of the illumination light coexist. Improvements such as application of contrast enhancement method to Dehaze [12], cooperation method with Retinex [17], edge preservation loss / coupling discrimination learning method [20], high resolution method by Laplacian Pyramid [21], etc. are progressing.

Dehazing with Improved Detail Visibility

Figure 1 shows the outline of the proposed model in which our joint sharpness-contrast enhancement pre-processor is placed in front of *Dehazing* to improve the visibility of details.

The objective of Dehazing is to restore the albedo $\boldsymbol{\rho}$ by unveiling the scattered *airlight* from a single camera image $\boldsymbol{I}$.

A hazed camera image $\boldsymbol{I}(z)$ is described by

$$\boldsymbol{I}(z) = \boldsymbol{J}(z)\boldsymbol{t}(z) + \boldsymbol{A}(1 - \boldsymbol{t}(z))$$
$$where,\ \boldsymbol{J}(z) = \boldsymbol{A}\boldsymbol{\rho}(z),\ \boldsymbol{t}(z) = exp^{-\beta d(z)} \quad (1)$$

where, σ denotes a scattering coefficient assuming Mie scattering

The 1st term denotes the direct transmission image from the scenic objects and the 2nd term means the *airlight* scattered from the *skylight* $\boldsymbol{A}$. The *skylight* $\boldsymbol{A}$ acts as a scene illumination and the *airlight* causes the hazy scene by veiling the direct transmission light. $\boldsymbol{J}(z)$ and $\boldsymbol{\rho}(z)$ denote the scene ***radiance*** and ***albedo***.

The scene transmittance $\boldsymbol{t}(z)$ is attenuated exponentially according to the scene depth $d(z)$. Note that $z=(x, y)$ denotes each pixel coordinates in the 2-D camera image $\boldsymbol{I}(z)$ corresponding to the objects placed at scene depth $d(z)$.

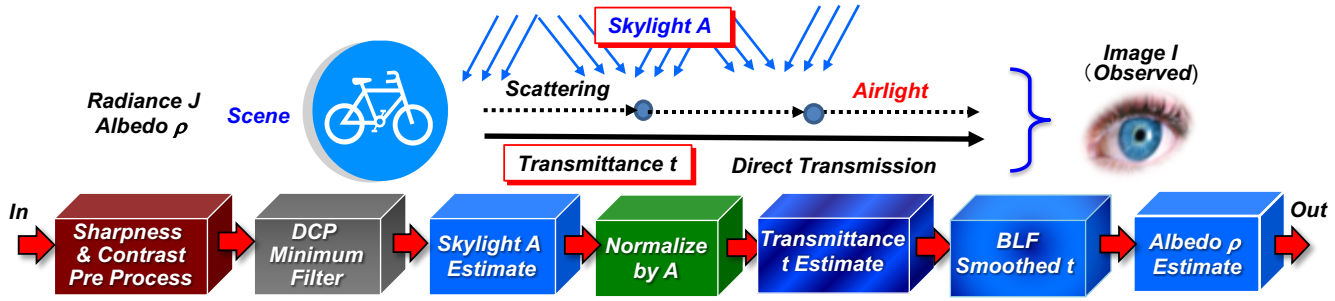

Figure 1. *Outline of proposed Dehazing system*

A key to restore the albedo $\boldsymbol{\rho}(z)$ is to estimate two unknown variables $\boldsymbol{A}$ *and* $\boldsymbol{t}(z)$. The author proposed a simple but effective solution in the previous paper [9].

The scene transmittance $\boldsymbol{t}(z)$ is attenuated exponentially according to the scene depth $d(z)$. Note that $z=(x, y)$ denotes each pixel coordinates in the 2-D camera image $\boldsymbol{I}(z)$ corresponding to the objects placed at scene depth $d(z)$.

A key to restore the albedo $\boldsymbol{\rho}(z)$ is to estimate two unknown variables $\boldsymbol{A}$ *and* $\boldsymbol{t}(z)$. The author proposed a simple but effective solution in the previous paper [9].

Since the *skylight* A equals the *airlight* coming from infinite $d=\infty$ with highest scattering, it's extracted from the luminance image $Y(z)$ of $I(z)$. Applying a local minimum filter to $Y(z)$, we get

$$Y^{dark}(z)=\left\{\min_{w\in\Omega(z)}\left(Y(w)\right)\right\} \tag{2}$$

The local ***min*** block filter substitutes the darkest value for pixel $\boldsymbol{w}$ inside each sub-divided block area Ω. As a result, the blocks for the scattered *airlight* hard to reach are omitted from the candidates.

Thus the *skylight* $\boldsymbol{A}$ is estimated by extracting the brighter area Ω_{Sky} and taking the average as

$$\tilde{\boldsymbol{A}}=\underset{w\in\Omega_{Sky}(z)}{mean}\left\{\boldsymbol{I}(w)\right\}\ for\ \Omega_{Sky}(z)=area\left\{Y^{dark}(z)\geq Y_H\right\} \tag{3}$$

Normalizing Eq. (1) by the estimated ***skylight*** $\tilde{\boldsymbol{A}}$, it's eliminated from the 2nd term as

$$I^C_{Norm}(z)=\frac{I^C(z)}{\tilde{A}^C}=\frac{J^C(z)}{\tilde{A}^C}t(z)+(1\text{-}t(z))\ for\ C=R,G,B \tag{4}$$

Operating DCP (Dark Channel Prior) [10] process on Eq. (4) and introducing a ***veiling factor*** $\varpi\ (0<\varpi<1)$, the scene transmittance $\boldsymbol{t}(z)$ is roughly estimated from the 2nd term in Eq. (1) as

$$\tilde{\boldsymbol{t}}(z)^{rough}(proposed)\cong 1\text{-}\varpi\left\{\min_{C\in\{R,G,B\}}\frac{\boldsymbol{I}^C(y)}{\boldsymbol{A}^C}\right\} \tag{5}$$

Because the scene transmittance should be spatially continuous and smooth, it's refined by *Bilateral Smoothing Filter* as

$$\tilde{\boldsymbol{t}}(z)^{smooth}=BilateralFilter[\tilde{\boldsymbol{t}}(z)^{rough}] \tag{6}$$

Once the ***skylight*** $\boldsymbol{A}$ and *scene* ***transmittance*** $\boldsymbol{t}(z)$ are estimated, the scene *albedo* is recovered from Eq. (1) as

$$\tilde{\boldsymbol{\rho}}(z)\cong\tilde{\boldsymbol{J}}(z)/\tilde{\boldsymbol{A}}=\left(\boldsymbol{I}(z)/\tilde{\boldsymbol{A}}\text{-}1+\tilde{\boldsymbol{t}}(z)\right)/\ Max\left[\tilde{\boldsymbol{t}}(z),\ t_0\right] \tag{7}$$

Where, *Max* [,] is a limiter to take $\tilde{t}(z)\geq t_0$ in case of the very low transmittance pixel point for the *albedo* $\tilde{\boldsymbol{\rho}}(z)$ not to diverge.

Usually, the veiling factor is set around ϖ=0.9 or higher to perfectly unveil the scattered *airlight*. While, the *ϖ-based Dehazing* works to regulate the scene transmittance $\tilde{t}(z)$ to at least 1-ϖ. By adjusting the veiling factor ϖ to the lower value, it'll be used for thin-hazed daily scenes. Figure 2 shows an example of adjusting the ϖ and applying it to the scenes of Tiananmen, where air pollution is severe, and Mt. Fuji, which is a few.

Figure 2*. De-hazed samples by tuning veiling factor* ϖ

Joint Sharpness-Contrast Enhancement

The visual effects of sharpness and contrast enhancement are confusing. The former emphasizes the high-frequency component that bears the contour and improves the appearance of details. The latter acts on mid- and low-frequency components other than details, emphasizing the difference in brightness between adjacent regions and facilitating the distinction between the background and the object.

Weber Contrast Enhancement

As a light/dark discrimination threshold, *Weber Fraction* is well known. It's given by $\Delta Y/\ Y$, where ΔY denotes luminance change in center C and Y is brightness of surround S. The C / S ratio reflects the light and dark perception characteristics of human vision.

Now, we define the *Weber Contrast Gain* W_G by taking the ratio of output *Weber Fraction* W_{out} vs. input *Weber Fraction* W_{in} as follows.

$$W_G(x,y) = W_{out} / W_{in} = \frac{dg(x,y)/g(x,y)}{df(x,y)/f(x,y)} \tag{8}$$

$f(x, y)$ and $g(x, y)$ denote input and output luminance images.

Here, replacing the surround luminance of $f(x, y)$ and $g(x, y)$ with their averages f_{ave} and g_{ave}, W_{in} and W_{out} are described by

$$W_{in}(x,y) = \left\{ f(x,y) - f_{ave}(x,y) \right\} / f_{ave}(x,y)$$
$$W_{out}(x,y) = \left\{ g(x,y) - g_{ave}(x,y) \right\} / g_{ave}(x,y) \tag{9}$$

Assuming the linear *Tone Reproduction Curve* $TRC(\bullet)$ between input and output we get

$$g_{ave}(x,y) = TRC\left\{ f_{ave}(x,y) \right\} \cong f_{ave}(x,y) \tag{10}$$

Since the average f_{ave} is given by a *Gaussian Convolution* with *Medium* size luminance surround $f_{ave} \approx S_M$, then the contrast enhanced output image g^{Cont} to keep W_G at a constant value of $W_G \cong \alpha\ (>1)$ is calculated as follows.

$$\mathrm{g}^{\mathrm{Cont}}(x,y) = \alpha f(x,y) - (\alpha - 1) S_M(x,y)$$
$$S_M(x,y) = G_M(x,y) * f(x,y) \tag{11}$$

where, G_M denotes *Gaussian function* with standard deviation σ_M and $*$ means Convolution integral.

Sharpness Enhancement

As an analogy of thermal diffusion, image blurring is modeled by the following partial differential equation.

$$\partial f / \partial t = k(\partial^2 f / \partial x^2 + \partial^2 f / \partial y^2) \tag{12}$$

Considering that the original image $f(0)$ without blur at time $t=0$ equals a blurred image $f(\Delta t)$ after $t=\Delta t$ elapses due to diffusion, the following is obtained with *Taylor* expansion near $t=0$ as

$$f(\Delta t) = f(0) + (\partial f / \partial t)\Delta t + \frac{1}{2}(\partial^2 f / \partial t^2)\Delta t^2 + \cdots \tag{13}$$

Ignoring the second and subsequent terms and setting the blur constant as $k\Delta t = \beta - 1$, then substituting Eq. (12) for , the sharpened image $g^{Sharp} = f(0)$ is given by

$$\mathrm{g}^{sharp}(x,y) \cong f(x,y) - (\beta - 1)\nabla^2 f(x,y) \tag{14}$$

Eq. (14) represents well-known image sharpening process with *USM* (*Unsharp Mask*) or *Laplacian 2nd. derivative operator.*

Since the *2nd. derivative* may be described by the difference between the center pixel f and near surround f_{ave}, we can use and is given by a *Gaussian Convolution* with a *small* size luminance surround $f_{ave} \approx S_S$.

Thus a sharpened image with enhance factor $\beta > 1$ is reduced to the following simple formula.

$$\mathrm{g}^{sharp}(x,y) \cong \beta f(x,y) - (\beta - 1) S_M(x,y)$$
$$S_M(x,y) = G_M(x,y) * f(x,y) \tag{15}$$

Here, it can be seen that the Eq.(15) has the same format as Eq.(11). The difference between the two lies in the luminance peripheral field, where contrast uses *Medium* size S_M to emphasize intermediate spatial frequency components, while sharpness uses *Small* size S_S to emphasize high spatial frequency components. This suggests that both functions may be *combined* into one.

Fusion of Sharpness and Contrast Enhancement

Figure 3 shows an outline of fusion model. Here, it is assumed that the input luminance image f is subjected to first *contrast* and next *sharpness* enhancement in sequence.

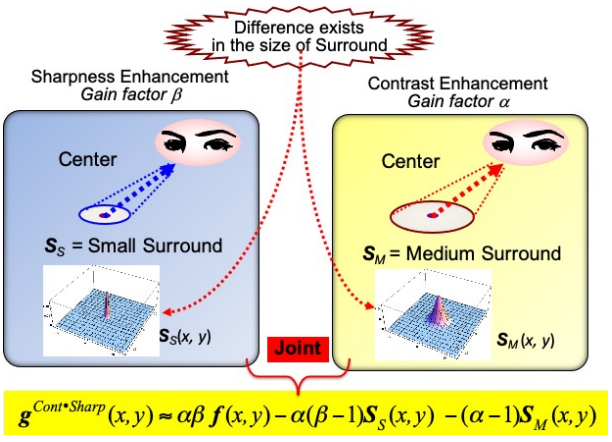

Figure 3. Rough Sketch of Joint Sharpness-Contrast Enhance Model

First, *contrast* enhanced image g^{Cont} is already described in Eq. (11). If we continue to sharpen this, connecting the equations

$$g^{Cont \bullet Sharp}(x,y) = \beta g^{Cont}(x,y) - (\beta\text{-}1) S_S(x,y)$$
$$S_S(x,y) = G_S(x,y) * g^{Cont}(x,y) \tag{16}$$

Substituting Eq.(11) into Eq.(16) and rearranging, we get

$$\begin{aligned} g^{Cont\bullet Sharp}(x,y) &= \alpha\beta f(x,y) \\ &-\alpha(\beta\text{-}1)G_S(x,y)*f(x,y) \\ &-(\alpha\text{-}1)\beta G_M(x,y)*f(x,y) \\ &+(\alpha\text{-}1)(\beta\text{-}1)G_S(x,y)*\{G_M(x,y)*f(x,y)\} \end{aligned} \tag{17}$$

Now, the fourth term of Eq. (17) requires a computation costs, because the convolution integral with the Gaussian function in the medium area is further subjected to the *double Convolution Integral* with the small region for input image *f*.

Since the fourth term is the size *M* peripheral field of input image *f* with a small Gaussian blur added, the convolution integral by $\boldsymbol{G}_S$ may be omitted in consideration of the scale M > S.

Now, omitting the first *Gaussian Convolution*, we get

$$G_S(x,y)*\{G_M(x,y)*f(x,y)\} \approx G_M(x,y)*f(x,y) \tag{18}$$

Finally we get a simplified approximation solution

$$\begin{aligned} g^{Cont\bullet Sharp}(x,y) &\approx \alpha\beta f(x,y) \\ &-\alpha(\beta\text{-}1)S_S(x,y) - (\alpha\text{-}1)S_M(x,y) \end{aligned} \tag{19}$$

Figure 4 shows an example of the emphasis effect using the Log-F Sine MTF Chart. For the MTF degraded camera image (b), α contributes to the enhancement of the intermediate frequency and β contributes to the enhancement of the high spatial frequency region. This result tells us that the appropriate value of emphasis coefficient exists around α=β=1.2~1.3 based on *HVSS* (*Human Visual Sub System*) characteristics.

Now, the input image $\boldsymbol{I}$ is processed in the order of Contrast ⇒ Sharpness ⇒ Dehaze, and the output $\boldsymbol{O}$ is obtained like as

$$\boldsymbol{O}(x,y)=\boldsymbol{Dehaze}\{\boldsymbol{Sharpness}\{\boldsymbol{Contrast}\{\boldsymbol{I}(x,y)\}\}\} \tag{20}$$

Experimental Results

The performance of proposed model is compared with typical other models as shown in Figure 5 and Figure 6.

Figure 5 shows a comparison of the Hazy scenes in New York, which are cited in many papers. Gardran looks good at first glance, but the proposed method is clearly the best way to restore the details of the windows in a close-up. Bermann fails to estimate the skylight.

The superiority of the proposed method was verified in most cases measured by the ***index*** γ newly introduced as described below.

Figure 6 is the most recent examples. Since the grand truth scenes without haze are unknown, it is difficult to evaluate, but the proposed model looks to be visually superior in detail.

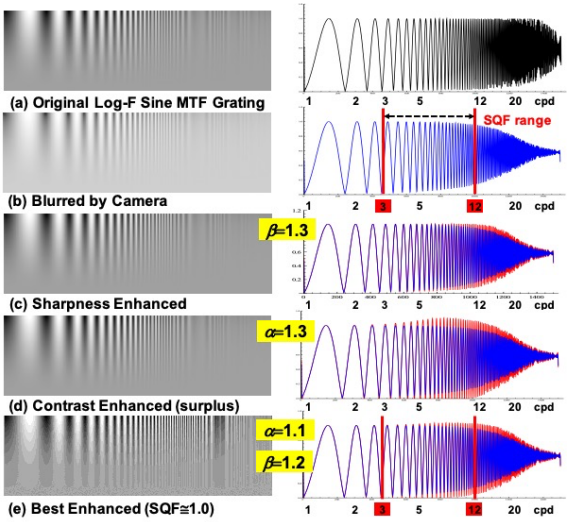

Figure 4. Sharpness-Contrast Enhancement Effect with Log-F Sine MTF

Evaluations

Fourier Analysis for Sharpness & Contrast Effects

Since the high-frequency components in images attenuate with blur, a simple way for image sharpness assessment is to measure the attenuation of the spectral distribution.

The magnitude of image spectrum $M(\omega)$ is known to fall exponentially with reciprocal of frequency ω like as

$$M(\omega) \propto \omega^{-\gamma} \tag{21}$$

Taking the *log*arithm of $M(\omega)$

$$log\{M(\omega)\} \propto -\gamma log(\omega) \tag{22}$$

Now we can get a single sharpness index γ from the line slope.

It's said that the smaller the index γ, the sharper the image and blurred if $\gamma > 1$.

Applying *Fourier DCT transform* $\mathcal{F}$ to the sharpened image, the 2D spectral distribution is obtained as

$$\mathcal{I}_{sharp}(\omega_x, \omega_y) = \mathcal{F}[I_{sharp}(x,y)] \tag{23}$$

For simplicity, the 2D distribution is converted to 1D by

$$\mathcal{I}_{sharp}(\omega_x, \omega_y) \rightarrow \mathcal{I}_{sharp}(\omega) \; for \; \omega = \sqrt{\omega_x{}^2 + \omega_y{}^2} \tag{24}$$

The $log\{\mathcal{I}_{sharp}(\omega)\}$ is fitted by a straight line with slope γ by

$$log\{\mathcal{I}_{sharp}(\omega)\} \cong K - \gamma\omega, K = const \tag{25}$$

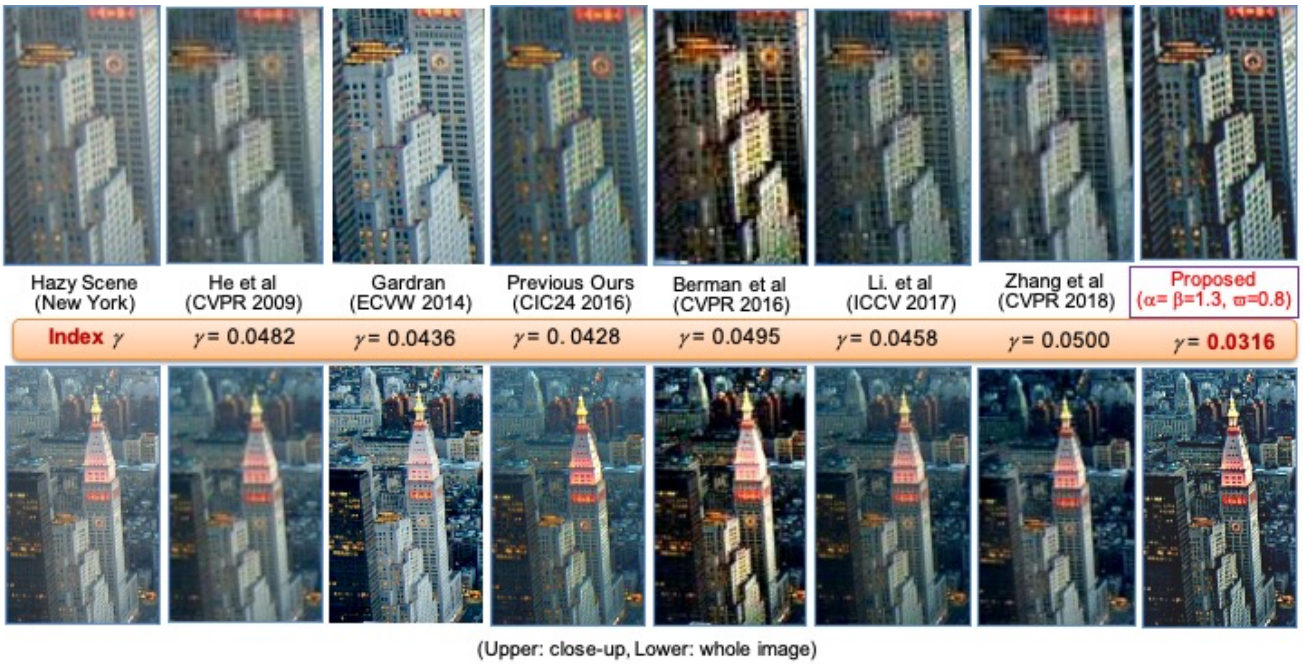

Figure 5. Comparative examples of typical Dehazing models for Hazy New York City and evaluated sharpness index g

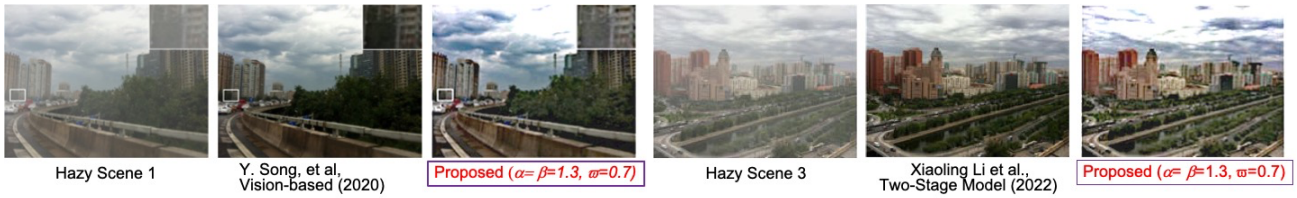

Figure 6. A comparison with most recent model vs. Ours

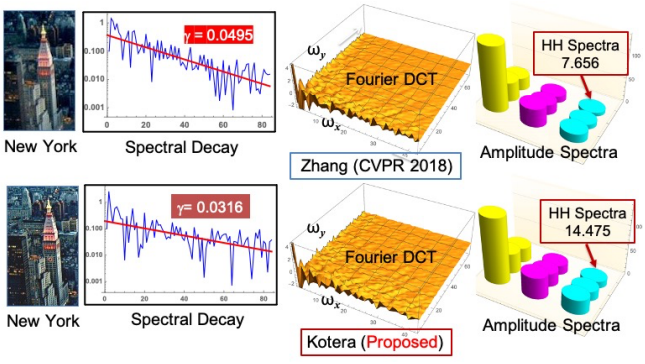

Figure 7. Overview of Fourier Spectral Decay in comparison of two models.

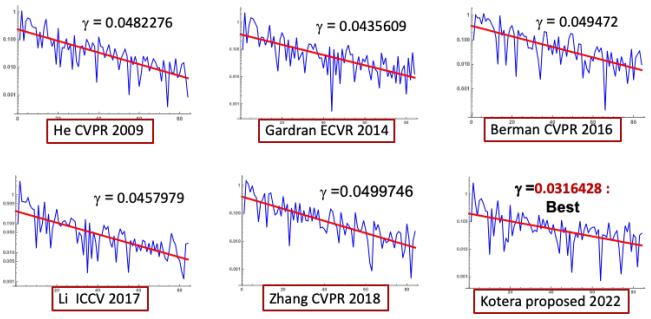

Figure 8. Effects in Sharpness & Contrast enhancement pre-process

Figure 7 shows an overview of the *Fourier* DCT spectral attenuation to evaluate the effect of Sharpness & Contrast enhancement pre-process by comparing Zhang vs our methods using the example of hazy New York in Figure 5. Since the index g of our system is obviously smaller than that of Zhang, the sharpness is superior. This is also supported by the fact that the high-frequency component HH of the Fourier spectrum is larger.

Figure 8 illustrates a comparative example of Fourier spectral attenuations in typical Dehazing models. The proposed model resulted in the best with the smallest value of index g .

Measuring Dehazing Effects by Gamut Volume

As a simple way to measure to the Dehazing effect, we examined the rate of increase in *color gamut volume* before and after.

Here, the *CIELAB* color distribution is analyzed using *PCA* (Principal Component Analysis) and estimated the approximate ellipsoidal volume of the color solid as follows.

$$\begin{aligned} &\mathcal{Vol}\left\{I(z)^{LAB}\right\} \cong (4\pi/3)\sqrt{\lambda_1}\sqrt{\lambda_2}\sqrt{\lambda_3} \\ &\boldsymbol{\lambda} = \{\lambda_1,\lambda_2,\lambda_3\} = \mathcal{Eigenvalue}\left\{I(z)^{LAB}\right\} \end{aligned} \tag{26}$$

Figure 9 shows an example how the Gamut Volume is incresed by our proposed method before and after Dehazing.

In this sample, the volume is increased to 1.5 times by Dehazing only, and more increased by 0.38 times with Sharpness & Contrast pre-process totally resulting in 1.88 times.

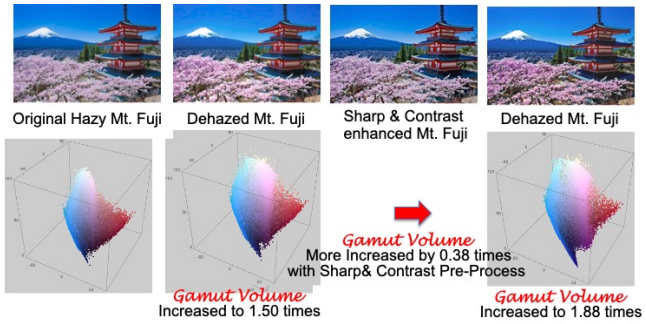

Figure 9. An example of Gamut Volume increased by Dehazing

Conclusions

In this paper, the improvement of the dehazing method to improve poor visibility caused by fog, haze and air pollution is taken up from the viewpoint of urban traffic and safe navigation of aircraft.

Specifically, preprocessing that simultaneously enhances sharpness and contrast is preceded before Dehazing.

Since the grand truth scene is unknown, until now, any assessment of the effectiveness of haze removal has not been made. Here, we introduced two numerical scales, (1) the index g as an attenuation coefficient of the Fourier spectrum, and (2) the degree of increase in the color gamut volume, as a method for evaluating the effect of improving the visual appearance.

It was verified by applying it to real specific images.

Now, the center of air pollution in the world has moved from India and Mongolia to Nepal, Qatar and Saudi, but still serious.

The development of such as real-time Dehazing processor [25] is awaited for safe driving of cars and aircraft and prevention of traffic accidents. It is expected that more advanced and practical Dehazing technology will be born in the near future.

References

[1] E. H. Land and J. J. McCann, "Lightness and Retinex Theory", Jour. Optical Society of America., 61, 1–11, 1971.

[2] J. J. McCann, "Retnex at 40", Jour. Electronic Imaging, 13(1), 6-145, 2004.

[3] J. J. McCann, "Retinex at 50 color theory and spatial algorithms, a review," Jour. Electronic Imaging, 26(3), 031204-1-14, 2017.

[4] D. Jobson et al, "Properties and performance of a center/surround retinex", IEEE Trans., Image Processing, 6, 451-462, 1997.

[5] G. Woodell et al, "Advanced image processing of aerial imagery Visual Information Processing XV, Proc. SPIE 6246, 2006.

[6] S. Narasimhan and S. K. Nayar, "Vision and the Atmosphere", Jour. Computer Vision, 48(3), 233-254, 2002.

[7] R. Fattal, "Single Image Dehazing", ACM SIGGRAPH, 27, 1-9, 2008.

[8] R. Tan, "Visibility in Bad Weather from a Single Image", Proc. IEEE Computer Vision and Pattern Recognition, Anchorage, 1- 8, 2008.

[9] J. Tarel and N. Hautiere, "Fast visibility restoration from a single color or gray level image", Proc. 12th International Conference on Computer Vision, 2201-2208, 2009.

[10] K. He et al., "Single image haze removal using dark channel prior", Proc. IEEE Computer Vision and Pattern Recognition, 1956-1963, 2009.

[11] J. Yu et al. "Physics-based Fast Single Image Fog Removal", Proc. 10th. International Conference on Signal Processing, 1048-1052, 2010.

[12] A. Galdran et al., "A Variational Framework for Single Image Dehazing", Computer Vision, ECCV Workshops, 259–270, 2014.

[13] H. Kotera, "Unveiling PM 2.5 Pollution Layer for Viewing Clear Scenes", in 22 nd. Color and Imaging Conference, 59-64, 2014.

[14] H. Kotera, "UNVEILING PM 2.5 POLLUTION LAYER FOR LOOKING CLEar SCENES", Proc. International Workshop on Image Electronics and Visual Computing, 4B-4, 2014.

[15] H. Kotera, "Scene Color Correction with De-hazing Algorithm based on Atmospheric Scattering Model", Proc. 1st. International Conference on Advanced Imaging, T-101-02, 2015.

[16] H. Kotera, "Scene Color Correction Under Non-Uniform Spatial Illumination and Atmospheric Transmittance", in 24 th. Color and Imaging Conference, 300-305, 2016.

[17] V. J. W. Dravo and J. Y. Herdeberg, "Multiscale Approach for Dehazing Using the STRESS Framework", Jour. Imaging Sci. and Technol., 60 (1), 2016

[18] D. Berman et al., "Non-Local Dehazing", IEEE Conference on Computer Vision and Pattern Recognition, 1674-1682, 2016

[19] S. Lee et al., "Review on DCP Dehazing", Jour. Image and Video Processing, EURASIP, 1-24, 2016.

[20] He. Zhang and V. M. Patel, "Densely Connected Pyramid Dehazing Network", Proc. Computer Vision and Pattern Recognition, 3194- 3203, 2018.

[21] D. Engin et al., "Cycle-Dehaze: Enhanced Cycle GAN for Single Image Dehazing", Proc. IEEE Computer Vision and Pattern Recognition, 825-833, 2018.

[22] P. Perona and J. Malik, "Scale-Space and Edge Detection Using Anisotropic Diffusion", IEEE Trans. on *Pattern Analysis and Machine Intelligence,* 12,7, 629-639,1990.

[23] C. Tomasi and R. Manduchi, "Bilateral filtering for gray and color images", Proc. IEEE International Conference on Computer Vision, 839-846, 1998.[24] Y. Monobe et al., "Dynamic range compression preserving local image contrast for digital video camera", IEEEE Trans. on Consumer Electronics, 51,1, 1-11, 2005.

[25] Tan Zhiming et al., "Fast Single-image Defogging", Fujitsu, 64, 5, 523-528, 2013.

[26] H. Kotera, "Inverse-Scaled Lanczos Filtering for Image Sharpening", in 28 th. Color and Imaging Conference, 215-220, 2020.

Author Biography

Hiroaki Kotera *joined Panasonic in 1963. He received Ph.D. from Univ. of Tokyo. After worked at Matsushita Res. Inst. Tokyo during 1973-1996, he was a professor at Chiba University. He retired in 2006 and has been collaborating with Chiba University. He received 1993 IS&T honorable mention, 1995 SID Gutenberg prize, 2005 IEEE Chester Sall award, 2007 IS&T Raymond. C. Bowman award, 2009 SPSTJ and 2012 IIEEJ best paper awards. He is a Fellow of IS&T and IIEEJ.*